ORIGINAL RESEARCH

Characterization of Short Intense Pulsed Electrothermal Plasma Capillaries for Use as Fusion and Launchers Heat Flux Sources

Mohamed A. Abd Al-Halim · Mohamed A. Bourham

Abstract Electrothermal plasma sources operating in the confined capillary arc regime are characterized by the magnitude and shape of the discharge current. The desired plasma parameters at the source exit, especially the pressure and heat flux, are highly dependent on the arc due to the effect of the arc radiant energy that ablates the inner wall of the source. These sources have applications in fusion as drivers for pellet injectors and as high heat flux sources for fusion materials studies. The high-pressure high heat flux flow is also of application in mass accelerators and launch technology systems. The 1-D, time-dependent ETFLOW capillary code models the plasma generation and flow inside the capillary discharges and determines the plasma parameters. The input file to the code is the discharge current density providing the Joule heating in the energy equation. A circuit module has been developed and incorporated in the code to generate desired current shapes and magnitudes. The current pulse length was varied between 5 and 100 μs at constant amplitude of 50 kA, and then the pulse amplitude was varied between 10 and 200 kA at a constant pulse length of 20 μs. Increasing the pulse length while maintaining its amplitude increases the plasma density and the total ablated mass, which have accumulation behavior by increasing the pulse length, and subsequently increases the exit pressure from 60 to 410 MPa in the cases studied herein. The pressure increase

allows the thermalization of the plasma particles through more collisions, which reduces the plasma temperature by about 0.2 eV. The bulk velocity follows the trend of the plasma temperature, but at shorter pulse lengths the total ablated mass is lower and enables the plasma to carry the particles with increasing velocity. Increasing the pulse amplitude up to 200 kA increases the density to about 18 kg/m^3 and the bulk velocity, which varies between 6.1 and 10.7 km/s. A sharp increase in most plasma parameters occurs as a result of the increase in the pulse amplitude.

Introduction

Several theoretical and experimental studies were conducted on capillary discharges for their use as high heat flux sources for fusion studies and launch technology. A capillary discharge is, essentially, a small tubular configuration with an inner liner and two electrodes to conduct an arc discharge, which in turn ablates the surface of the liner and produces plasma.

Various material surfaces have been exposed to the heat flux in capillary discharge devices, like SIRENS and PIPE facilities to study their erosion behavior. Tested materials vary from pure metals and alloys, to refractory and specially coated materials, insulators and composites, and pure and composite graphite [1, 2]. The arc emits radiant energy and the formed dense plasma continues to radiate as a blackbody. Typical density of such plasmas is in the range of 10^{24}–10^{28} m^{-3} with typical temperature between 1 and 5 eV [3]. The reduction in surface erosion for a given incident radiant heat flux is due to the vapor shield effect,

M. A. Abd Al-Halim
Physics Department, Faculty of Science, Benha University, Benha 13518, Egypt
e-mail: mohamed.abdalhalim@fsc.bu.edu.eg

M. A. Bourham (✉)
Department of Nuclear Engineering, North Carolina State University, Raleigh, NC 27695-7909, USA
e-mail: bourham@ncsu.edu

where the energy transmission factor through the vapor shield may be as low as 5 % for increased heat flux, hence the net flux to the surface can be reduced due to the energy absorption in the vapor shield [3–5]. Electrothermal plasma sources have potential applications in fusion reactors as drivers for pellet injectors for fusion fueling and as high heat flux sources for fusion materials studies. The other application of capillary discharges is their use as igniters for the electrothermal-chemical (ETC) launchers. Ignition and control of the combustion of solid propellants requires pulsed power systems, which provide a high flexibility in pulse shape via pulse forming networks. In a series of studies a design of a system consisted of 540 kJ capacitive discharge modules with a maximum charging voltage of 30 kV each was studied. The pulse shape of each module can be adjusted by the selection of its lumped circuit elements and the capacitors [6]. The design of 120 kJ capacitor modules was investigated with energy density in the range between 0.8 and 1.0 MJ/m^3 [7] and others of up to 2.7 MJ/m^3 [8]. The performance of ETC launchers, all ET pellet accelerators for fusion fueling, and miniature space thrusters, is influenced by the time frame over which electric energy is deposited into the ET source [9]. Usually, the load resistance can be used to supply the required shape of the current pulse, and it can be calculated from the measured discharge current and voltage to develop an approximated model of the load resistance [10]. Several pulse power modules were constructed for the hyper velocity and ETC launch system in which inductors were utilized for the pulse shaping [11–13].

A 1-D time dependent model was developed to use the recovered Ohmic power input in the source term of the energy equation of an ET system, which allowed for the determination of the resistive component in capillary discharges [14]. The FNGUN finite difference based internal ballistics code has been used and concluded that there is a dependence of the overall system performance on the anticipated electrical behavior of the plasma and the electrical pulse shape [15]. A one-dimensional model for ablative capillary discharges has found that a maximum exit values of the parameters are, $T \approx 4.22$ eV, $\rho \approx 1.4$ kg/m^3, P = 210 MPa and velocity of about 15.8 km/s [16]. Also, a hydrodynamic model for electrical arc modeling was used to study the interaction between the electrical arc and the sidewall and found that the main mechanism at the sidewall was the photo ablation [17]. Modeling of ET devices was developed for the SIRENS and PIPE facilities using a 0-D, time-dependent code ZEUS [18], and a 1-D, time-dependent fluid dynamics code ODIN [19]. The code includes energy transport, equation of state, and electrical resistivity models. The wall material under high heat flux will usually lead to ablation and energy loss by axial convection transport in a cylindrical geometry. The scaling law of the transmission

factor was derived and used to determine a single value of the factor in the case of two time dependent experimental shots [20]. The 1-D model was further developed to include the non-ideality of the plasma "ETFLOW code" and the incorporation of the circuit model in the code [21, 22].

This study focuses on investigation of the effect of the current pulse shape and amplitude on the plasma parameters with the use of polyethylene as the inner ablating sleeve. The current pulse length was varied between 5 and 100 µs at constant amplitude of 50 kA to determine the plasma parameters dependence on the pulse length, and then the pulse amplitude was varied between 10 and 200 kA at a constant pulse length of 20 µs to determine the plasma parameters dependence on the pulse amplitude for short intense pulses.

Source Configuration and ETFLOW Code

Plasma in the electrothermal sources is generated by discharging a capacitor into the capillary, which in turn drives an arc through the capillary and radiates energy to the wall of the inner liner "sleeve" via blackbody radiation. The absorbed energy on the surface of the wall causes ejection of atoms followed by ionization and plasma generation [23]. The cascade of events continues as the temperature increases and the pressure builds. The arc plasma is found to be in local thermodynamic equilibrium condition LTE [24]. The plasma source in the breech consists of an insulating cylindrical sleeve made of an insulator such as Lexan polycarbonate and housed inside of a cylindrical metallic anode. The ablating sleeve may be polymeric such as polyethylene (PE) or Lexan, or ceramics such as aluminum oxide or boron nitride. Polyethylene was used as the ablating sleeve in this research.

Changing the value of the capacitance and the total circuit inductance can vary the pulse length, while changing the charging voltage and the total stray resistance
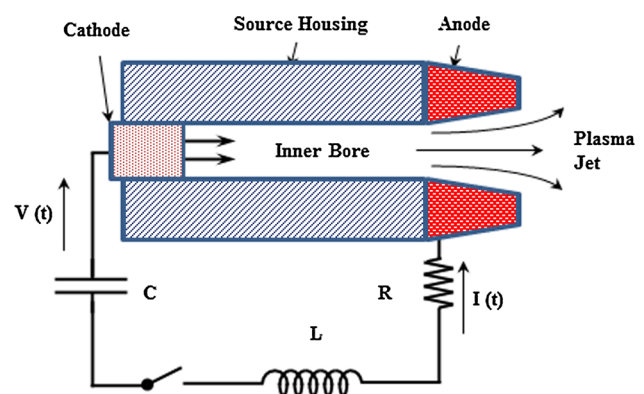

Fig. 1 Simplified drawing of an electrothermal (ET) plasma source

controls the pulse amplitude. A simple equivalent electric circuit of the electrothermal capillary discharge is shown in Fig. 1, which shows the main lumped circuit elements C, L and R. The RLC circuit model was built in the ETFLOW code to generate a current pulse according to the values of the circuit components. The circuit equation can be represented by $L\frac{dI}{dt} + RI = V - \frac{1}{C}\int I dt$ with the initial conditions at t = 0 to be $I = 0$, $\int I dt = 0$, $dI/dt = V/L$. A time increment δ is set to advance the time step as $t = t + \delta$, which is used to calculate the pulse magnitude at the selected total pulse length and hence $I = I + \delta(dI/dt)$ and $\int I dt = \int I dt + I\delta$.

The ETFLOW is a 1-D, time dependent code that models plasma formation and flow in electrothermal capillary plasma discharge sources. The system of governing equations is solved self-consistently to obtain the plasma parameters such as the plasma temperature and density, kinetic pressure, plasma velocity, total ablated mass, and plasma conductivity. The code is written in FORTRAN and runs in a VBA environment. The code has a circuit module to generate the pulse shape and amplitude. The basic equations are the conservation of mass, momentum, and energy with the detailed plasma models, Saha equation, and the equation of state, ionization, viscosity and electrical conductivity with both ideal and nonideal formalism. Full details of the complete set of equations are given elsewhere [19, 21].

Results and Discussion

Pulse Length Effect

Pulse length was varied from 5 to 100 μs at constant amplitude of 50 kA. The pulse length is varied in the code by controlling the circuit inductance and the capacitance. Figure 2 shows the effect of the pulse length variation on the maximum plasma temperature and the peak exit velocity. The exit bulk velocity increases from 7.2 km/s for a 5 μs pulse length to 8.2 km/s at 20 μs then decreases very slightly with increased pulse length up to 100 μs, it appears almost unchanged between 20 and 100 μs indicating that the increased pulse length didn't change the velocity. This result is consistent with previous work on the extended flattop pulse in which it was shown that that velocity remains almost unchanged [9]. The plasma temperature decreases with increased pulse length, however, the decrease is slight as it drops from 2.86 for 5 μs to 2.7 for 100 μs pulse length, which is also consistent with previous investigation of the extended flattop pulse [9]. The best fit shows that the temperature follows a logarithmic form $T_{(eV)} = 2.95 - 0.06 \, \ell n(\tau)_{\mu s}$. As the pulse length increases
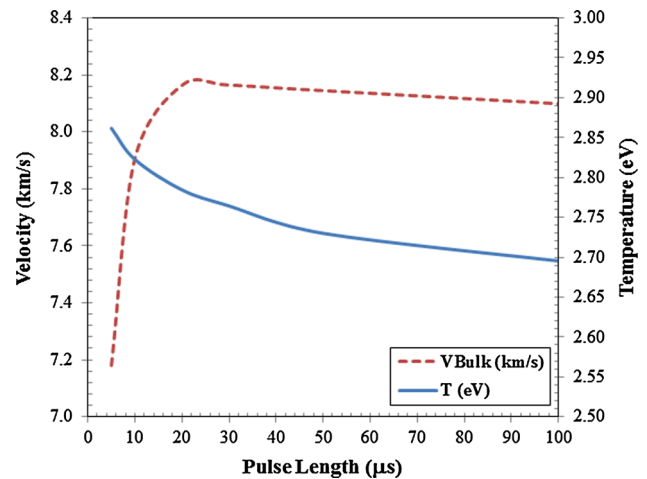

Fig. 2 Effect of pulse length on plasma temperature and the bulk velocity at the capillary exit

the total energy deposition increases but is distributed along the allowed time for the discharge. This is the reason about why the temperature did not vary too much (less than 0.2 eV). The temperature behavior indicates a near uniform radiant heat flux, unchanged over different pulse lengths.

Figure 3 shows the plasma peak exit pressure and the total ablated mass. The pressure increases from 60 to 410 MPa as the pulse length increases from 5 to 100 μs. The maximum pressure has an accumulation behavior and increases by increasing the pulse length, which allows for a longer time for surface ablation, and hence increases the total ablated mass. The pressure follows a logarithmic law $P_{(MPa)} = 119 \, \ell n(\tau)_{\mu s} - 137.3$, where τ is the pulse length. The increase in the plasma pressure allows thermalization of the plasma particles through more collisions, which results in reduction of the plasma temperature as previously seen from the temperature graph. The total ablated mass, which is the sum of all masses ablated in the discharge time, is increasing almost linearly with the increase in the pulse length; however, the best fit shows a power law $M_{(mg)} = 0.95 \, \tau_{(\mu s)}^{0.85}$. The total ablated mass can be compared to the sum of all particle densities (electrons, ions and neutrals) as will be discussed later on.

Figure 4 shows the peak plasma density and the peak number densities of electrons and the ions in their first and second ionization states. As previously mentioned, the plasma density is the sum of the total particle densities, electrons, ions and neutrals. The number density of individual particles increases with increased pulse length due to increased ablation and ionization. There is a tendency that the individual particle density tends to stay unchanged when the pulse length increases, which is attributed to the balance between the ionization and recombination rates. It
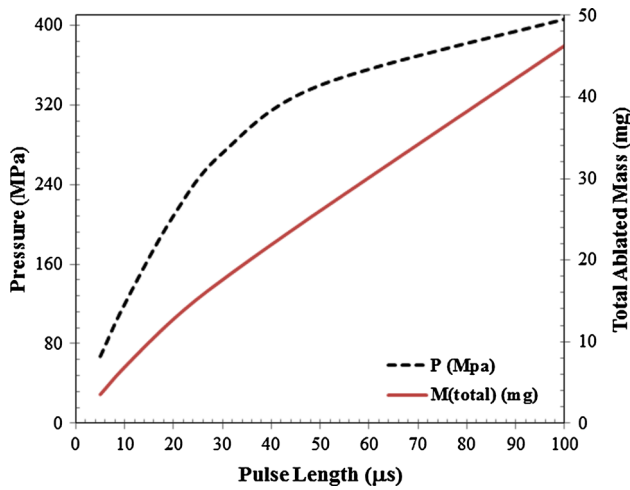
Fig. 3 Effect of pulse length on plasma pressure and the ablated mass at the capillary exit
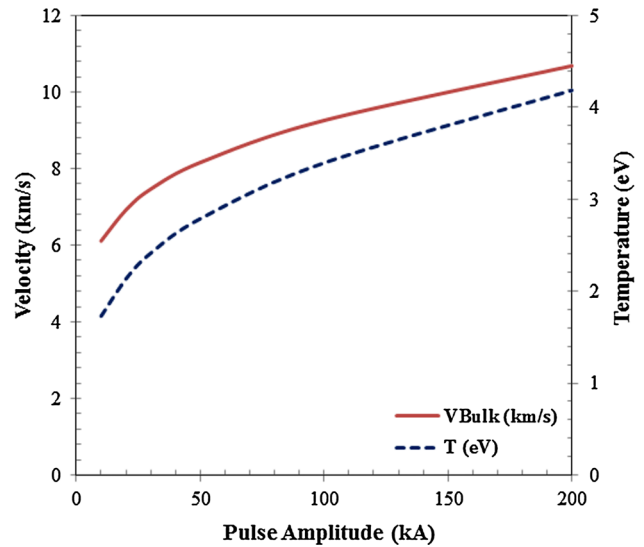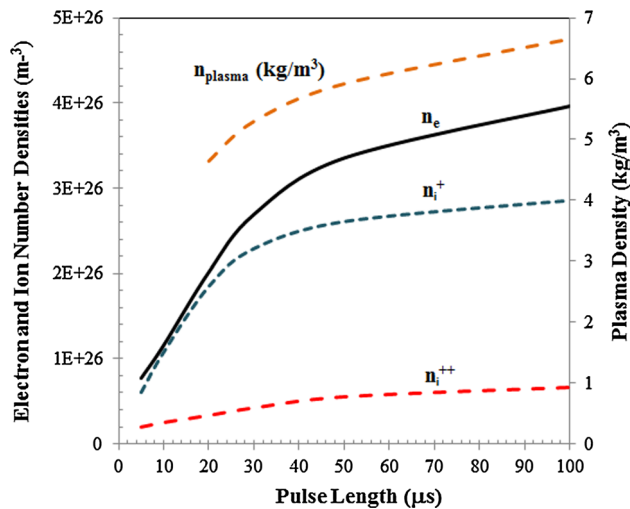

Fig. 4 Effect of pulse length on exit particle number density and total plasma density

is consistent with the previous investigation on extended flattop pulse where it was shown that the density levels off at longer pulse lengths [9]. The trend in the number density is similar to that of the pressure, as expected, due to the fact that the pressure is related to both the number density and the temperature. While the temperature stays almost unchanged, very slight drop with increased pulse length, however, the major effect on the pressure is the number density of the plasma particles. This also can be correlated to the total ablated mass, which is directly related to the total number of particles with their respective weights. The total mass will increase at a lower rate, which is of similar trend reported in the literature but with polyethylene as the liner of the capillary [25].

Fig. 5 Effect of pulse amplitude on plasma temperature and the bulk velocity at the capillary exit

Pulse Amplitude Effect

Pulse amplitude was varied from 10 to 200 kA at a constant pulse length of 20 µs, which is considered as an intense fast rise short pulse. The pulse amplitude is varied in the code by changing the resistance and mainly by charging voltage on the capacitor to change the net energy input to the capillary, while the pulse length was set to 20 µs based on controlling the values of the circuit elements (R, L and C). Increasing the charging voltage will increase the total energy supplied to the plasma particles per unit time, so since the pulse length is constant, the whole increment in the applied energy will appear as an increase in the peak plasma temperature as shown in Fig. 5, where the temperature rises to 4.2 eV for the 200 kA pulse. The temperature follows a power law $T_{(eV)} = 0.89 \, I_{(kA)}^{0.29}$, which correlates well with the scaling laws developed by Vergara [26]. Also shown in Fig. 5 is the exit plasma bulk velocity, which increases from 6.1 km/s for the 10 kA pulse to reach 10.7 km/s for the 200 kA pulse. The bulk velocity, in general, is proportional to the temperature as $v \propto T^{1/2}$, and hence it is expected that the trend in the velocity will follow the shape of the temperature, the best fit is also in a power law $v_{(km/s)} = 3.98 \, I_{(kA)}^{0.19}$. This behavior in the velocity variation with the increase in the current amplitude was experimentally observed and reported using black Lexan as the sleeve material and found that up to a maximum current of 200 kA a significant increase in the velocity can be achieved [27].

Figure 6 shows plasma peak exit pressure and the total ablated mass. As the pulse magnitude increases the total ablation increases, which also reflects on the pressure and the increase appears more linear with the pulse amplitude,
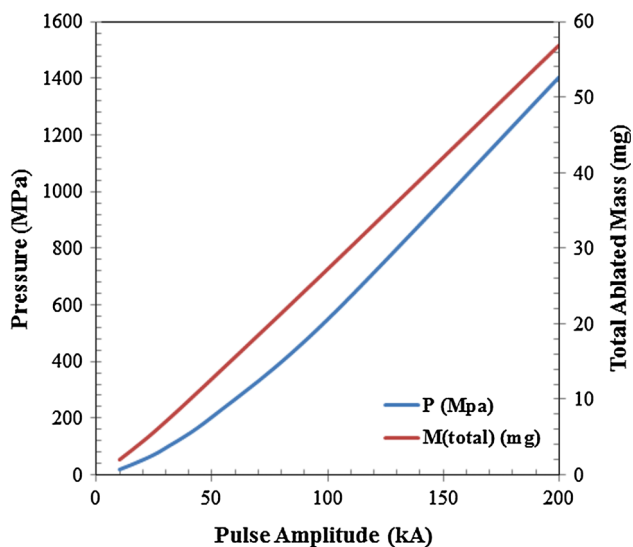
Fig. 6 Effect of pulse amplitude on plasma pressure and the ablated mass at the capillary exit

Fig. 7 Effect of pulse amplitude on exit particle number density and total plasma density

however, an actual best fit shows a power law $P_{(MPa)} = 0.69 I_{(kA)}^{1.44}$. The total ablated mass rises to 57 mg at 200 kA, which is not substantial in capillary discharges running at extended pulse lengths. The case of 50 kA at 100 μs pulse length (as previously shown in Fig. 3) shows 46.3 mg, however, the difference is in the short 20 μs pulse that provided a quick transient heat flux for the 200 kA case. The best fit for the ablated mass also follows a power law $M_{(mg)} = 0.16 I_{(kA)}^{1.12}$. The fitting of the pressure and the ablated mass are in good correlation with developed scaling laws [27]. A comparison between the calculated mass loss and the measured mass loss in the source section showed that the measured and calculated mass losses agreed fairly well for all input energies [5, 19, 20]. Similar trends were reported for experiments with nylon as a sleeve material [28], polyethylene sleeve [27], and black Lexan [29] but with lower values of the ablated mass. The lower values in the case of the reported black Lexan could result from calculating the dissociation energy according to the bonds energies, which is higher than the energy required to dissociate the polyethylene. This means that lower energies than the dissociation energy is used to break some bonds and then transfer the layer from solid to vapor stated at which it is partially ionized and dissociate. This was supported by researches for Lexan materials in which the studies proved that ablation could take place in lower value than the calculated ones for the dissociation energies [30, 31]. The very high exit pressure is important for various applications in launch systems and can provide great acceleration to pellet injection for fusion reactors fueling. The pressure approaches 1,400 MPa for the 200 kA pulse in 20 μs, and similar result for achieving very high
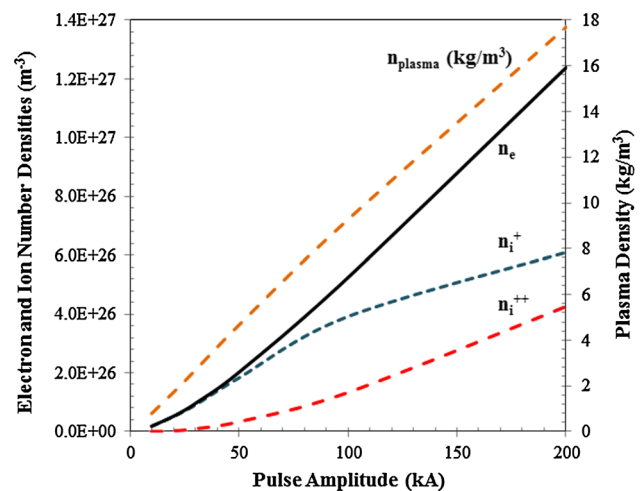
pressures with high discharge currents was reported in the literature for the case of nylon and boric acid capillaries [32].

Figure 7 shows the peak plasma density and the peak number densities of electrons and the ions in their first and second ionization states. It is clear that the electron number density, as well as the total plasma density, and the total ablated mass are in direct proportion with the pulse amplitude. The plasma density reached about 17.7 kg/m^3 for the 200 kA pulse amplitude. The number density of the individual particles increases with increased pulse amplitude due to increased ablation and ionization. Of importance is the increase in the ionic concentration for both first and second ionizations, which can be of substantial effect in ionic impact on propellants in ETC systems.

Conclusions

Effect of pulse length and amplitude was investigated to determine their effect on the plasma parameters in confined capillary discharges. Of specific interest was the investigation of the pulse length at constant peak discharge current of 50 kA. Also the effect of a short 20 μs pulse with different amplitudes up to 200 kA was studied. The circuit model was used to generate these pulse shapes and the input current into the ETFLOW code to calculate the plasma parameters with a special interest in these parameters at the capillary exit.

At constant pulse amplitude of 50 kA, the plasma temperature slightly decreased from 2.86 to 2.7 as the pulse length increased from 5 to 100 μs, while the plasma exit pressure varied between 60 and 410 MPa. As the pulse length increases, the total energy deposited increases;

however, it is distributed along the entire discharge time. The plasma density and the total ablated mass also increased as ablation has increased. The increase in the plasma pressure allows thermalization of the plasma particles through more collisions, which results in reduction of the plasma temperature. The bulk velocity increases from 7.2 km/s for a 5 μs pulse length to 8.2 km/s at 20 μs then decreases very slightly with increased pulse length up to 100 μs. The total ablated mass follows a power law with the pulse length, while the pressure and velocity follow a logarithmic law.

At constant short pulse length of 20 μs and increased pulse amplitude up to 200 kA, it was shown that the densities and the total ablated mass are in direct proportion with the pulse amplitude. The temperature, velocity, pressure and ablated mass are all following a power law with the current amplitude. The density reached 17.7 kg/m^3 while the total ablated mass reached about 57 mg at 200 kA pulse amplitude. The bulk velocity varied between 6.1 and 10.7 km/s, which indicate an exit hyper velocity suitable for several launch applications including acceleration of pellets for fusion reactors fueling.

References

1. M.A. Bourham, J.G. Gilligan, M.L. Huebschman, D. Lianos, P.D. Aaltos, Review of component erosion in electric launcher technology. IEEE Trans. Magn. **31**, 678 (1995)
2. M. Keidar, I.D. Boyd, Ablation study in the capillary discharge of an electrothermal gun. J. Appl. Phys. **99**, 053301 (2006)
3. M.A. Bourham, O.E. Hankins, J.G. Gilligan, J.D. Hurley, J.R. Earnhart, Comparative study of component erosion for electromagnetic and electrothermal launchers. IEEE Trans. Magn. **29**, 1107 (1993)
4. J. Gilligan, M. Bourham, O. Hankins, O. Auciello, S. Tallavarjula, R. Mohanti, Studies to reduce material erosion in electrothermal launchers. IEEE Trans. Magn. **27**, 476 (1991)
5. M.A. Bourham, O.E. Hankins, O. Auciello, J.M. Stock, B.W. Wehring, R.B. Mohanti, J.G. Gilligan, Vapor shielding and erosion of surfaces exposed to a high heat load in an electrothermal accelerator. IEEE Trans. Plasma Sci. **17**, 386 (1989)
6. H.G. Wisken, F. Podeyn, H.G. Weise, A 540 kJ modular capacitive pulsed power supply system for basic investigation on ETC performance. IEEE Trans. Magn. **35**, 394 (1999)
7. H.G. Wisken, H.G. Weise, Capacitive pulsed power supply systems for ETC guns. IEEE Trans. Magn. **39**, 501 (2003)
8. H.G. Wisken, F. Podeyn, H.G. Weise, High energy density capacitors for ETC gun applications. IEEE Trans. Magn. **37**, 332 (2001)
9. A.L. Winfrey, M. Abd Al-Halim, A.V. Saveliev, J.G. Gilligan, M.A. Bourham, Enhanced performance of electrothermal plasma sources as fusion pellet injection drivers and space based minithrusters via extension of a flattop discharge current. J. Fusion Energ. **32**, 371 (2013)
10. Y.H. Lee, K.J. Park, J.W. Jung, Load resistance estimation in ETC experiments. IEEE Trans. Magn. **39**, 248 (2003)
11. Y.S. Jin et al., Performance of 2.4-MJ pulsed power system for electrothermal-chemical gun application. IEEE Trans. Magn. **39**, 235 (2003)
12. Y.S. Jin et al., Design and performance of a 300 kJ pulsed power module for ETC application. IEEE Trans. Magn. **37**, 165 (2001)
13. H.S. Lee et al., Evaluation of a RVU-43 switch as the closing switch for a modular 300 kJ pulsed power supply for ETC application. IEEE Trans. Magn. **37**, 371 (2001)
14. M.R. Zaghloul, M.A. Bourham, J.M. Doster, Semi-analytical modelling and simulation of the evolution and flow of ohmically-heated non-ideal plasmas in electrothermal guns. J. Phys. D Appl. Phys. **34**, 772 (2001)
15. C.C.H. Guyott, The pulse shape requirements of an ETC gun. IEEE Trans. Magn. **31**, 56 (1995)
16. D. Zoler, D. Saphier, R. Alimi, A numerical study of the evolution of plasma parameters in an ablative capillary discharge for a two-pulse form of energy input. J. Phys. D Appl. Phys. **27**, 1423 (1994)
17. E. Domejean, P. Chevrier, C. Fievet, P. Petit, Arc-wall interaction modelling in a low-voltage circuit breaker. J. Phys. D Appl. Phys. **30**, 2132 (1997)
18. J. Gilligan, R. Mohanti, Time dependent numerical simulation of ablation controlled arcs. IEEE Trans. Plasma Sci. **18**, 190 (1990)
19. J.D. Hurley, M.A. Bourham, J.G. Gilligan, Numerical simulation and experiment of plasma flow in the electrothermal launcher SIRENS. IEEE Trans. Magn. **31**, 616 (1995)
20. R.B. Mohanti, J.G. Gilligan, Time dependent simulation of the plasma discharge in an electrothermal launcher. IEEE Trans. Magn. **29**, 585 (1993)
21. A.L. Winfrey, M. Abd Al-Halim, A.V. Saveliev, J.G. Gilligan, M.A. Bourham, A study of plasma parameters in a capillary discharge with calculations using ideal and non-ideal plasma models for comparison with experiment. IEEE Trans. Plasma Sci. **40**, 843 (2012)
22. R.B. Mohanti, J.G. Gilligan, M.A. Bourham, Time dependent simulation of weakly nonideal plasmas in electrothermal launchers. Phys. Fluids B **3**, 3046 (1991)
23. J.P. Sharpe, Particulate generation during disruption simulation on the SIRENS high heat flux facility, Ph. D. Dissertation, North Carolina State University, Raleigh, NC, USA (2000)
24. B.L. Lambert, Effects of incorporation of a new model for electron-ion collision frequency in an electrothermal plasma, MNE Thesis, North Carolina State University, Raleigh, NC, USA (2000)
25. L. Veron, P. Noiret, S. Roux, Experimental ablation processes study on an electrothermal launcher, in *Proc. 12th IEEE int. pulsed power conf.*, Monterey, USA, June 27–30 1995, 2, 1291–1295 (1995)
26. P.P. Vergara, Development of scaling laws for electrothermal plasma sources with geometry variables, MS Thesis, North Carolina State University, Raleigh, NC, USA (2013)
27. B. Dirr, Experimental investigation of a small bore plasma armature rail launcher at high current densities. IEEE Trans. Magn. **31**, 273 (1994)
28. M. Rott, The plasma-gun augmented electrothermal accelerator. IEEE Trans. Magn. **27**, 601 (1991)
29. M. Keidar, I.D. Boyd, A. Williams, R. Beyer, Ablation study in a capillary sustained discharge. IEEE Trans. Magn. **43**, 308 (2007)
30. F.D. Witherspoon, R.L. Burton, S.A. Goldstein, Railgun experiments with Lexan insulators. IEEE Trans. Plasma Sci. **17**, 353 (1989)
31. L.D. Jones, F.E. Karasz, Heat of fusion of Lexan polycarbonate. J. Polym. Sci. B Polym. Lett. **4**, 803 (1966)
32. P. Kovitya, Ablation-stabilized arcs in nylon and boric acid tubes. IEEE Trans. Plasma Sci. **PS-15**, 294 (1987)